

Edith Cowan University

Research Online

Research outputs 2014 to 2021

2021

Numerical assessment of the overall heat transfer and pressure drop performances of an aqueous ammonia base-nanofluids in rectangular microchannel heat sinks

Ahmed Mohammed Adham

Hussein A. Mohammed
Edith Cowan University

Follow this and additional works at: <https://ro.ecu.edu.au/ecuworkspost2013>



Part of the [Engineering Commons](#)

Adham, A.M., & Mohammed, H.A. (2021). Numerical assessment of the overall heat transfer and pressure drop performances of an aqueous ammonia base-nanofluids in rectangular microchannel heat sinks. *Journal of Mechanical Engineering Research and Developments*.44 (4), pp.373-380.

<https://jmerd.net/04-2021-373-380/>

This Journal Article is posted at Research Online.

<https://ro.ecu.edu.au/ecuworkspost2013/10295>

Numerical assessment of the overall heat transfer and pressure drop performances of an aqueous ammonia base-nanofluids in rectangular microchannel heat sinks

Ahmed Mohammed Adham[†], Hussein A. Mohammed[‡]

[†] Department of Mechanical and Energy Engineering Techniques, Erbil Technical Engineering College, Erbil Polytechnic University, Erbil, 44001, Iraq.

[‡] School of Engineering, Edith Cowan University (ECU), Joondalup WA 6027, Australia

*Corresponding author email: ahmed.adham@epu.edu.iq; ahamed.adham@gmail.com

ABSTRACT

In this paper, the thermal and hydrodynamic performances of an aqueous ammonia base-nanofluid ($\text{Al}_2\text{O}_3\text{-NH}_3(\text{aq})$) cooled in a rectangular microchannel heat sink was numerically investigated. The range of Reynolds number used in the investigation were between 140-1400. In order to assess the performance of the system during the employment of the proposed nanofluid, H_2O and $\text{Al}_2\text{O}_3\text{-H}_2\text{O}$ were also tested and their performances were compared to $\text{Al}_2\text{O}_3\text{-NH}_3(\text{aq})$ performance in terms of thermal resistance and pressure drop. Results from the simulation showed that the proposed nanofluid outperformed pure water and slightly higher than $\text{Al}_2\text{O}_3\text{-H}_2\text{O}$ in terms of thermal resistance (for $\text{Re} = 1400$, 0.0474, 0.0449 and 0.04647 $^\circ\text{K/W}$ for H_2O , $\text{Al}_2\text{O}_3\text{-H}_2\text{O}$ and $\text{Al}_2\text{O}_3\text{-NH}_3(\text{aq})$, respectively). However, it exceeds the performance of both pure water and $\text{Al}_2\text{O}_3\text{-H}_2\text{O}$ in terms of pressure drop (for $\text{Re} = 1400$, 785288, 911217, 753591 Pa for H_2O , $\text{Al}_2\text{O}_3\text{-H}_2\text{O}$ and $\text{Al}_2\text{O}_3\text{-NH}_3(\text{aq})$, respectively). The key findings from the current study may be used to attract more research about the proposed nanofluid to be used in the cooling process of microchannel heat sinks.

KEYWORDS

$\text{Al}_2\text{O}_3\text{-NH}_3(\text{aq})$, Numerical simulation, thermal resistance, ammonia.

INTRODUCTION

In the modern era, the requirement of having electronic devices able to perform multi-functions simultaneously is inevitable. This led to the invention of a very powerful electronic chips which allows the electronic devices to perform very efficiently without any noticeable delay [1]. On the other hand, these electronic chips produce huge amount of excessive heat compared to their sizes (up to 790 W/cm^2 [2]) which should be efficiently dissipated. Since the pioneer work of Tuckerman and Pease [2] which employed the concept of micro-electronic mechanical system (MEMS) to investigate the capabilities of microchannel heat sink to dissipate heat generated by these electronic chips, many researchers have attempted to increase the thermal performance of microchannel heat sinks [3-8]. Nowadays, researchers have looked into developing the heat transfer performance of microchannel heat sinks by utilizing liquids with suspended nanoparticles called nanofluids [9]. These nanofluids provide better thermal behavior compared to classical used coolants [10]. With the recent progress in nanotechnology, homogeneous (stable) nanofluids which overcome the issue of sedimentation and therefore passage clogging are available [11]. Lee and Mudawar [12] experimentally investigated the use of $\text{Al}_2\text{O}_3\text{-H}_2\text{O}$ with 2% volume fraction in rectangular microchannel heat sink. Enhancement in the overall heat transfer performance was noted specially in the laminar entrance region.

Koo and Kleinstreuer [13] numerically simulated the heat transfer process of $\text{CuO-H}_2\text{O}$ and CuO-ethylene in rectangular microchannel. They concluded that with a 4% volume fraction nanofluid, better heat transfer was performed. Mohammed et al. [14] employed numerical method (FVM) to explore the effect of different nanoparticles type on the overall thermal and hydrodynamic performances of triangle microchannel heat sink. Diamond- H_2O , Ag- H_2O , Diamond-Oil and Diamond-glycerin nanofluids were investigated. Diamond- H_2O and Ag- H_2O showed better performance in terms of thermal resistance and pressure drop compared to the other

nanofluids used. Halelfadl et al. [15] studied the overall performance of aqueous carbon nanotubes base nanofluid in rectangular microchannel. Optimization results showed that using CNT base nanofluid significantly lowered the overall thermal resistance compared to pure water. Mohammad Kalteh [16] studied the effects of nanoparticle types, base fluid, volume fraction on the overall performance of microchannel heat sink. Nine different nanoparticles (Al_2O_3 , CuO , Cu , Fe , Au , Ag , TiO_2 , SiO_2 and Diamond), Three different base fluids (water, ethylene glycol and engine oil) were studied. It was observed that the Diamond- H_2O performed better thermal performance compared to the aforementioned nanofluids. Shahsavari et al. [17] studied the effect of connecting holes on the overall performance of microchannel heat sinks using silver-water nanofluids.

Entropy generation behaviors were examined under laminar flow conditions. Results from the study showed that the connecting holes have increased the heat transfer when Reynolds number was between 500 to 2000. Vinoth and Sachuthanathan [18] investigated experimentally the heat transfer and fluid flow performances of a nanofluid-cooled microchannel heat sink under different channel geometries namely, pentagonal and triangular cross-sections. Water was the base fluid and different nanoparticles were used such as (CuO , Al_2O_3 and $\text{Al}_2\text{O}_3/\text{CuO}$ as a hybrid nanoparticles). Results from this study showed that pentagonal cross-section outperformed the triangular in terms of the thermal resistance when the hybrid nanofluid was used. According to the above literature, the effect of using different nanoparticles on the overall thermal performance of microchannel heat sinks were extensively studied. However, the effect of different base fluids has not received the same amount of attention from the researchers as it can be seen that there are only few base fluids were mostly used (H_2O , ethylene glycol and oil). Therefore, this paper will aim to propose a new base fluid namely (Aqueous ammonia) to be used in the preparation of the nanofluids. The mixture rate of the ammonia-water solution was 5:95. This mixture rate was taken into consideration in this study because it provides better thermal performance than pure water [19]. Furthermore, a comparative study will be carried out to explore the thermal and hydrodynamic performances of the microchannel heat sink cooled by the nanofluids with ammonia-water solution as a base fluid.

Mathematical Modelling

The physical model of the current study is shown in Fig. 1. To obtain the solution and to minimize the time required to solve the problem, one channel will be considered based on the fact that the entire system is symmetric as shown in Fig. 2.

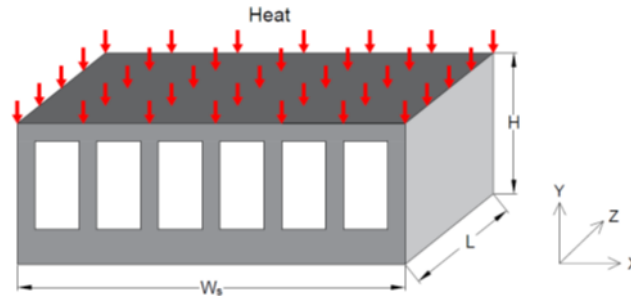


Figure 1. Schematic diagram of the microchannel heat sink.

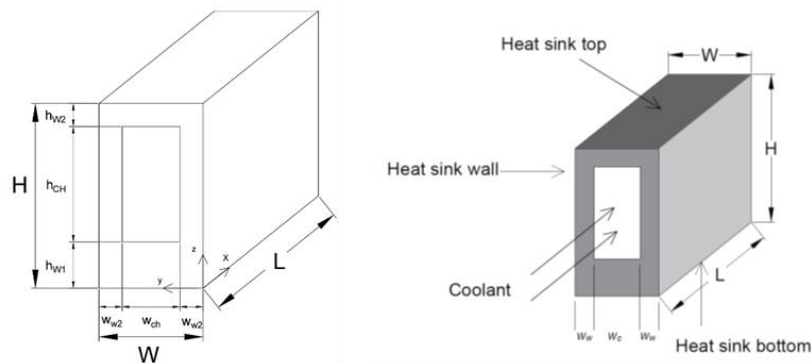


Figure 2. One channel calculation domain.

In order to facilitate the solution, the following assumptions were made:

1. The thermophysical properties of the coolant are constant.
2. Steady state, single phase, laminar and incompressible fluid flow are considered.
3. Heat loss to the surrounding is neglected.

Heat flux of (900000 W/m²) is exerted on the top surface of the microchannel heat sink and it is uniformly distributed. The governing equations for this case are as follows:

The continuity equation:

$$\frac{\partial u}{\partial x} + \frac{\partial v}{\partial y} + \frac{\partial w}{\partial z} = 0 \quad (1)$$

The momentum equations:

$$\rho \left(u \frac{\partial u}{\partial x} + v \frac{\partial u}{\partial y} + w \frac{\partial u}{\partial z} \right) = -\frac{\partial P}{\partial x} + \mu \left(\frac{\partial^2 u}{\partial x^2} + \frac{\partial^2 u}{\partial y^2} + \frac{\partial^2 u}{\partial z^2} \right) \quad (2)$$

$$\rho \left(u \frac{\partial v}{\partial x} + v \frac{\partial v}{\partial y} + w \frac{\partial v}{\partial z} \right) = -\frac{\partial P}{\partial y} + \mu \left(\frac{\partial^2 v}{\partial x^2} + \frac{\partial^2 v}{\partial y^2} + \frac{\partial^2 v}{\partial z^2} \right) \quad (3)$$

$$\rho \left(u \frac{\partial w}{\partial x} + v \frac{\partial w}{\partial y} + w \frac{\partial w}{\partial z} \right) = -\frac{\partial P}{\partial z} + \mu \left(\frac{\partial^2 w}{\partial x^2} + \frac{\partial^2 w}{\partial y^2} + \frac{\partial^2 w}{\partial z^2} \right) \quad (4)$$

The energy equation:

$$\rho C_p \left(u \frac{dT}{dx} + v \frac{dT}{dy} + w \frac{dT}{dz} \right) = k \left(\frac{d^2 T}{dx^2} + \frac{d^2 T}{dy^2} + \frac{d^2 T}{dz^2} \right) \quad (5)$$

The following hydrodynamic boundary conditions are applied:

- i. At the surfaces of the channel wall, $u = v = w = 0$.
- ii. At the channel inlet, $u = \text{const.}$, $T = T_{in}$ and $z = 0, P = P_m$.
- iii. At the channel outlet, $z = L, P = P_{ou}$.
- iv. For the thermal boundary conditions, all walls are assumed to be isolated except the top wall of the heat sink (channel top wall) where constant heat flux is applied:

$$q'' = k_s \frac{\partial T_s}{\partial z} \quad (6)$$

In order to determine the overall performance of the system, the total thermal resistance can be calculated as:

$$R_{th} = \frac{T_{max} - T_{min}}{q'' A_s} \quad (7)$$

The pumping power can be calculated as:

$$P_p = G \cdot \Delta P$$

The inlet temperature of the coolant is assumed to be constant and equal to 293 °K. The inlet velocity of the coolant can be determined from:

$$u = \frac{Re \times \mu_f}{\rho d_h} \quad (9)$$

Dimensions and thermophysical properties

In Table 1, the dimensions used to draw the microchannel heat sink were provided. Table 2 provides the properties of the structural material of the microchannel heat sink along with the properties of the coolants used in the current study. The properties of the nanofluids were calculated based on volume fraction of 2%. Because of the low volume fraction considered, the nanofluid is homogeneous.

Table 1. Dimensions of the rectangular microchannel.

H (μm)	W (μm)	h_{w1} (μm)	h_{w2} (μm)	h_{ch} (μm)	w_{ch} (μm)	$w_{w1,2}$ (μm)	d_h (μm)
900	100	450	270	180	57	21.5	86

Table 2. Properties of the structural material and coolants.

Material	ρ (kg/m^3)	K (W/m.K)	C_p (J/kg.K)	μ (kg/m.s)
Silicon	2330	148	712	----
H_2O	997.7	0.6	4178.9	0.000949
$\text{Al}_2\text{O}_3\text{-H}_2\text{O}$	1057.636	0.64882	3925.48	0.00105315
$\text{Al}_2\text{O}_3\text{-NH}_3(\text{aq})$	1038.82	0.627	4187.9	0.0009556

RESULTS AND DISCUSSIONS

In order to validate the model, results from the current simulation was validate with the results given by Shah and London [20] for the average Nusselt number along the microchannel length as shown in Fig.3.

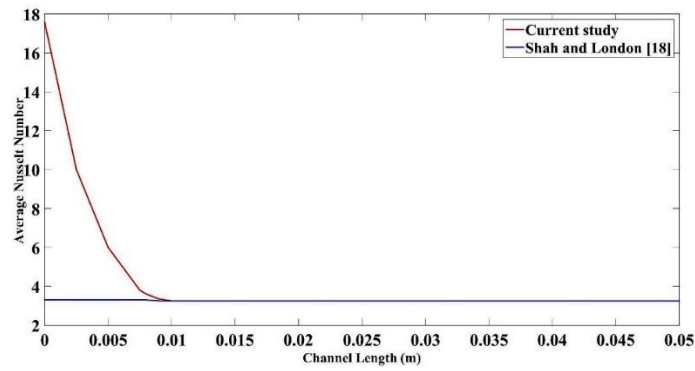


Figure 3. Validation of current model with Shah and London [18].

The results show adequate agreement between the results obtained from the current simulation and Shah and London work. Therefore, the model can be used further to study the overall thermal performance of the considered system. In addition, a grid independence test was carried out and the results are listed in table 3. It can be inferred from that, mesh size has a marginal effect on the results and increasing the mesh size will only increase the calculation time. Therefore, second case was chosen to carry out the simulation.

Table 3. Grid independence test results.

No.	Elements number	T(at the $L = 0.01$) $^{\circ}\text{K}$
1	69600	301.22
2	129688	301.395
3	212744	301.412

Figure (4), illustrates the temperature variation at the channel top wall where the constant heat flux is applied. It can be seen that the proposed nanofluid behaves better than pure water and slightly higher than $\text{Al}_2\text{O}_3\text{-H}_2\text{O}$ in terms of the temperature distribution along the channel length.

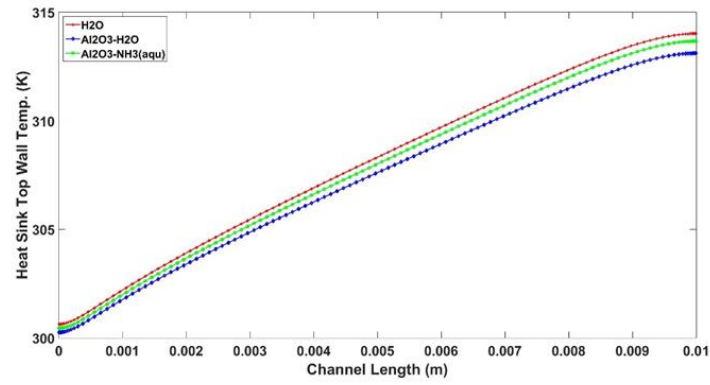


Figure 4. Temperature variation for all fluids along the channel length.

In fig. (5), the total thermal resistance for different Reynolds number is given. It can be seen that the total thermal resistance of $\text{Al}_2\text{O}_3\text{-NH}_3(\text{aqu})$ performs better than pure water. This can be attributed to the fact that the proposed nanofluid possesses better thermophysical properties compared to pure water. More specifically, better thermal conductivity and specific heat capacity. These aforementioned properties have an impact of the conductive and capacitive thermal resistances which ultimately reduces the total thermal resistance.

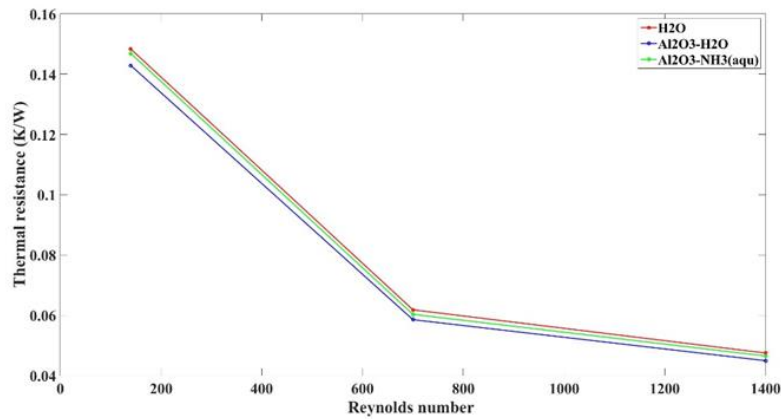


Figure 5. Total thermal resistance vs. Reynolds number for different coolants.

The total pressure drop for different Reynolds number is given in fig. (6). It can be seen that with the increase in Reynolds number, the total pressure drop is increases. This can be related to the increase in the inlet velocity of the coolant in the channel. Figure (6) also provide another interesting result which is clearly shows that the $\text{Al}_2\text{O}_3\text{-NH}_3(\text{aqu})$ outperformed the pure water and $\text{Al}_2\text{O}_3\text{-H}_2\text{O}$ in terms of the pressure drop (has lower pressure drop which consequently lowers the pumping power demand).

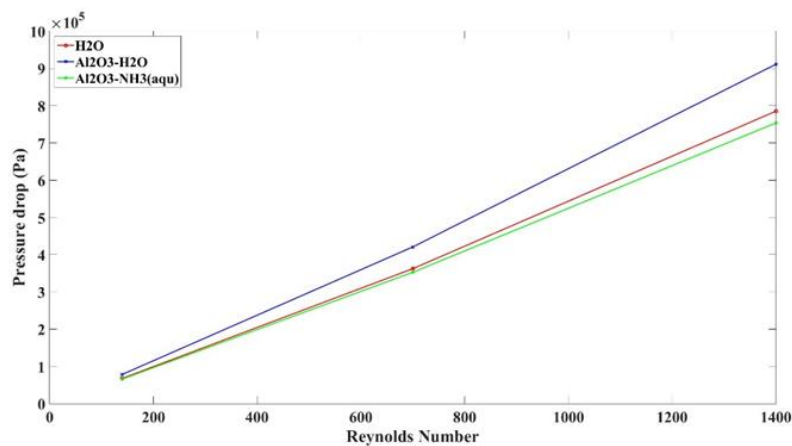


Figure 6. Pressure drop vs. Reynolds number for all coolants

In this part of the results, the performance of the coolant in terms of Nusselt number and friction factor will be presented. Figure (7) depicts the surface Nusselt number along the channel length. It can be seen that the Nusselt number is increases with the increase in Reynolds number. This can be attributed to the increase in the velocity as a result of the increase in Reynolds number which ultimately leads to enhance the convection heat transfer in the channel.

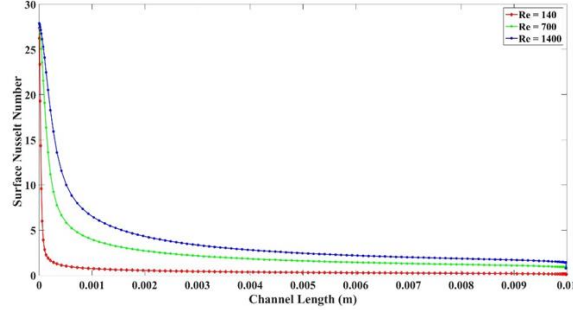


Figure 7. Surface Nusselt number vs. Channel length for different Reynolds numbers.

In fig. (8), the variation in the friction factor along the channel length is shown. It can clearly be seen that the friction factor is decreasing with the increase in the Reynolds number. Also, the difference between friction factor values associated to the $Re = 700$ and 1400 is slightly lower for $Re = 1400$. The trend seen coherent with the trend seen before for the friction factor behavior for different Reynolds number.

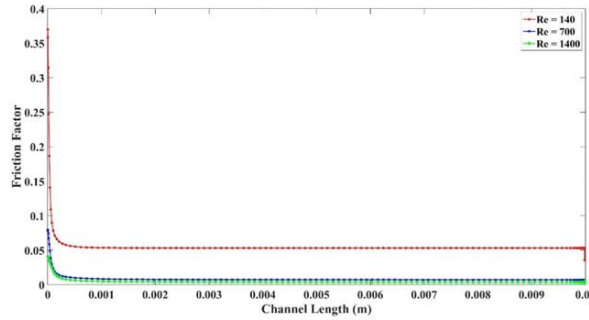


Figure 8. Friction factor vs. channel length for different Reynolds number.

Figure (9) shows the temperature contours for Re of (140, 700 and 1400). It can be seen that the maximum temperature occurs at the end of the channel top because the heat flux was applied at the top surface of the heat sink and hence the channel top. With the increase in Reynolds number (increase in velocity), more heat was dissipated and the maximum temperature area approaches it minimum.

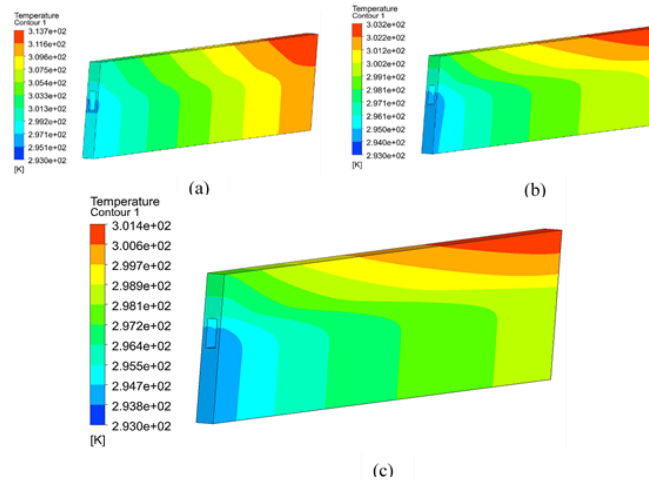


Figure 9. Temperature contours for (a) $Re = 140$, (b) $Re = 700$ and (c) $Re = 1400$.

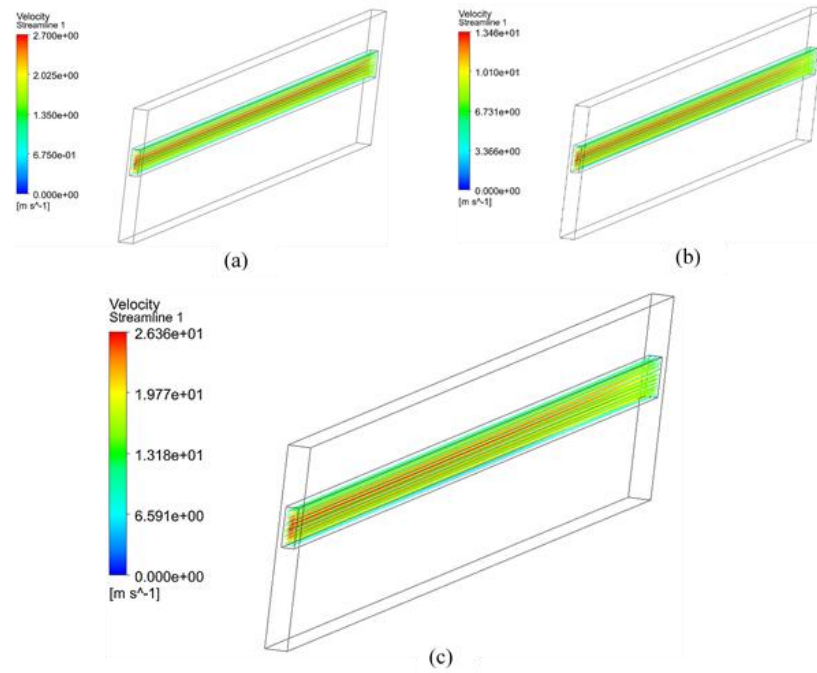


Figure 10. Velocity streamlines for (a) $Re = 140$, (b) $Re = 700$ and (c) $Re = 1400$.

The velocity streamlines for different Reynolds number are shown in fig. (10). It can be seen that the minimum velocity occurs at the channel walls. This is due to the non-slip condition applied at these walls. On the other hands, the maximum velocity can be noted at the center of the channel. This is because the boundary layer effects get to be weaker as we go towards the center of the channel therefore, the free stream velocity (maximum) value can be seen at the center of the channel.

CONCLUSIONS

The overall performance of an ammonia-water mixture base nanofluid was numerically investigated. The effects of the temperature distribution, Nusselt number and friction factor along the channel length were studied. In terms of thermal resistance, it was found that $Al_2O_3-NH_3$ has lowered the thermal resistance compared to pure water by 2.1 %. On the other hand, it was found that the pressure drop was lowered by 4 % and 17 % compared to H_2O and $Al_2O_3-H_2O$, respectively. In addition, the surface Nusselt number increases as the Reynolds number is increasing. Friction factor was decreasing along the channel length with the increase of Reynolds number. Therefore, and based on these facts, the proposed nanofluid can be an attractive subject for more research to explore its capabilities in the field of microchannel heat sink.

REFERENCES

- [1] A.M. Adham, N.M. Ghazali, and R. Ahmad, "Thermal and hydrodynamic analysis of microchannel heat sinks: A review", *Renewable and Sustainable Energy Reviews*, Vol. 21, Pp. 614-622, 2013.
- [2] D.B. Tuckerman, and R. F. W. Pease, "High-performance heat sinking for VLSI", *Electron. Device Lett*, IEEE Vol. 2, No. 5, Pp. 126-129, 1981.
- [3] A. Abdollahi, H.A. Mohammed, Sh. M. Vanaki, A. Osia, and M.R. Golbahar Haghighi, "Fluid flow and heat transfer of nanofluids in microchannel heat sink with V-type inlet/outlet arrangement", *Alexandria Engineering Journal*, Vol. 56, Pp. 161-170, 2017.
- [4] P.C.M. Kumar, and C.M.A. Kumar, "Numerical evaluation of cooling performances of semiconductor using CuO /water nanofluids", *Heliyon*, Vol. 5, Pp. e02227, 2019.
- [5] I.A. Ghani, N.A. Che Sidik, and N. Kamaruzaman, "Hydrothermal performance of microchannel heat sink: The effect of channel design", *International Journal of Heat and Mass Transfer*, Vol. 107, Pp. 21-44, 2017.

- [6] E. Manay, E.F. Akyurek, and B. Sahin, "Entropy generation of nanofluid flow in a microchannel heat sink", *Results in Physics*, Vol. 9, Pp. 615-624, 2018.
- [7] A.M. Sahar, M.R. Ozdemir, E.M. Fayyadh, J. Wissink, M.M. Mahmoud, and T.G. Karayiannis, "Single phase flow pressure drop and heat transfer in rectangular metallic microchannels", *Applied Thermal Engineering*, Vol. 93, Pp. 1324-1336, 2016.
- [8] J. Bowers, H. Cao, G. Qiao, Q. Li, G. Zhang, E. Mura, and Y. Ding, "Flow and heat transfer behavior of nanofluids in microchannels", *Progress in Natural Science: Materials International*, Vol. 28, Pp. 225-234, 2018.
- [9] M.U. Sajid, and H.M. Ali, "Thermal conductivity of hybrid nanofluids: A critical review", *International Journal of Heat and Mass Transfer*, Vol. 126, Pp. 211-234, 2018.
- [10] W. Arshad, and H.M. Ali, "Experimental investigation of heat transfer and pressure drop in a strigth minichannel heat sink using TiO₂ nanofluid", *International Journal of Heat and Mass Transfer*, Vol. 110, Pp. 248-256, 2017.
- [11] M.L. Zorab, and A.M. Adham, "Entropy generation minimization of microchannel heat sink using nanofluids as a coolant", *Journal of Mechanical Engineering Research and Development*, Vol. 43, Pp. 150-164, 2020.
- [12] J. Lee, and I. Mudawar, "Assessment of the effectiveness of nanofluids for single-phase and two-phase heat transfer in micro-channels", *International Journal of Heat and Mass Transfer*, Vol. 50, Pp. 452-463, 2007.
- [13] J. Koo, and C. Kleinstreuer, "Impact analysis of nanoparticle motion mechanisms on the thermal conductivity of nanofluids", *International Communications in Heat and Mass Transfer*, Vol. 32, Pp. 1111-1118, 2005.
- [14] H.A. Mohammed, P. Gunnasegaran, and N.H. Shuaib, "The impact of various nanofluids types on triangular microchannel heat sink performance", *International Communications in Heat and Mass Transfer*, Vol. 38, Pp. 767-773, 2011.
- [15] S. Halefadi, A.M. Adham, N.M. Ghazali, T. Mare, P. Estelle, and R. Ahmad, "Optimization of thermal performance and pressure drop of rectangular microchannel heat sink using aqueous carbon nanotubes based nanofluid", *Applied Thermal Engineering*, Vol. 62, Pp. 492-499, 2014.
- [16] M. Kalteh, "Investigating the effect of various nanoparticle and base liquid types on the nanofluids heat and fluid flow in microchannel", *Applied Mathematical Modelling*, Vol. 37, Pp. 8600-8609, 2013.
- [17] A. Shahsavar, S. Entezari, I.B. Askari, and H.M. Ali, "The effect of using connecting holes on heat transfer and entropy generation behaviors in a micro channels heat sink cooled with biological silver/water nanofluids", *International Communications in Heat and Mass Transfer*, Vol. 123, Pp. 104929, 2021.
- [18] R. Vinoth, and B. Sachuthananthan, "Flow and heat transfer behavior of hybrid nanofluis through microchannel with two different channels", *International Communications in Heat and Mass Transfer*, Vol. 123, Pp. 105194, 2021.
- [19] N.H.M. Razif, A.M.I. Mamat, I. Lias, and W.A.N.W. Mohamed, "Thermophysical properties analysis for ammonia-water mixture of an organic Rankine cycle", *Jurnal Teknologi*, Vol. 8, Pp. 13-17, 2015.
- [20] R.K. Shah, A.L. London, "Laminar flow forced convection in ducts: T. F. Irvine, J. P. Hartnett a source book for compact heat exchanger analytical data", Elsevier Science, 2014.